Prompt reactivity determination in a subcritical assembly through the response to a Dirac pulse

F. Perdu, J.M. Loiseaux, A. Billebaud, R. Brissot, D. Heuer, C. Le Brun, E. Liatard, O. Meplan, E. Merle, H. Nifenecker, et al.

Prompt reactivity determination in a subcritical assembly through the response to a dirac pulse

F. Perdu, J.M. Loiseaux, A. Billebaud, R. Brissot, D. Heuer,

C. Lebrun, E. Liatard, O. Meplan, E. Merle, H. Nifenecker,

J. Vollaire

Institut des Sciences Nucléaires

53, avenue des Martyrs

38026 Grenoble Cedex

tel. 04.76.28.41.50

fabien.perdu@m4x.org

Abstract

The full understanding of the kinetics of a subcritical assembly is a key issue for its online reactivity control. Point kinetics is not sufficient to determine the prompt reactivity of a subcritical assembly through the response to a dirac pulse, in particular in the cases of a large reflector, a small reactor, or a large subcriticality.

Taking into account the distribution of intergeneration times, which appears as a robust characteristic of each type of reactor, helps to understand this behaviour.

Eventually, a method is proposed for the determination of the prompt reactivity. It provides a decrease rate function depending on the prompt multiplication coefficient $k_{\text{eff}}^{\text{p}}$. Fitting a measured decrease rate with this function, calculated once for the

reactor, gives the true value of $k_{\mathrm{eff}}^{\mathrm{p}}$. The robustness of the method is tested.

Key words: reactor, kinetics, subcriticality, neutron pulse, prompt jump, reflector

PACS: 28.41.Ak

1   Introduction

In the context of ADS studies and MUSE 4 experiments, where very short pulses of neutrons are delivered in the middle of the core of a small experimental fast neutron reactor (MASURCA), various methods for determining the parameters of a subcritical assembly submitted to a pulsed source are discussed.

While the delayed neutron proportion β_{eff} can be extracted from the slow evolution of the reaction rate between the pulses [5], the reactivity determination is still a major concern.

There are two main definitions of the multiplication coefficient k. The source multiplication coefficient, k_{s}, is linked to the multiplication of a particular source, and can be deduced from the total power of the reactor at equilibrium. [7][8]. Its definition depends on the definition of a source neutron, which can be very difficult when the initial particles are protons, for example in an ADS[10]. The effective multiplication coefficient, k_{eff}, is, on the contrary, an intrinsic characteristic of the reactor. It corresponds to the multiplication of the stabilized fission distribution, many generations after the source has been turned off. That is why this coefficient is considered to govern the safety of the reactor. During the operation of a power ADS reactor, one could imagine a case where k_{eff} rises while the source is progressively poisoned, in such a way

2

that k_s and the total power do not change. In that case, a small reactivity insertion may become sufficient to cause an accident, while no warning signal can be seen from the power of the reactor. That is why a safety requirement for operating any subcritical reactor will probably be to keep it below a maximum k_{eff}. The ability to monitor this quantity continuously in order to detect any abnormal evolution is thus a central issue.

Unfortunately, the presence of the source hides the characteristics related to the effective (late) fission distribution. There are two ways of getting rid of the influence of the source. The first one is to turn it off and deduce k_{eff} from the fluctuations at zero power. In this case, k_{eff} is not known in the real conditions of operation.

The second one, which is chosen here, is to study the decrease following a source pulse. The usual method which consists in measuring the decrease rate at long time scales (typical of delayed neutrons) is only precise for reactivities smaller than β_{eff}, which is not compatible with ADS reactivities. Moreover, it requires the knowledge of β_{eff} and a very low intrinsic source. That is why we chose here to deal rather with the prompt decrease following the pulse, which is today accessible to experiment. This choice leads to the measurement of prompt k_{eff} rather than total k_{eff}. But this information is sufficient as we can measure β_{eff} by other means. What is more, the subcriticality will in general be far greater than β_{eff}, and the precise knowledge of β_{eff} will not be essential.

We used only Dirac pulses in the present studies. However, this method can be applied for all other types of source pulses, simply by convolving every quantity measured with the actual pulse shape.

The purpose of this work is to determine the relevant quantity that should

be measured, and possibly simulated, in order to get a robust evaluation of prompt k_{eff}. In the following $k_{\text{eff}}^{\text{p}}$ will always be the prompt effective multiplication coefficient.

2 The one group point kinetics and its failure

In the one group point kinetics calculations, the spatial and spectral distribution of neutrons is assumed to be a constant in time, which implies that every cross section averaged over the flux is constant [3][4][5][6].

2.1 The prediction

Without a source, the number of neutrons $N(t)$ satisfies

$$\frac{dN}{dt} = \left(\nu_{\text{p}}\langle\Sigma_{\text{f}}\rangle - \left(\langle\Sigma_{\text{f}}\rangle + \langle\Sigma_{\text{c}}\rangle + DB^2\right)\right) N\langle v\rangle$$

where ν_{p} is the average number of prompt neutrons produced by fission, $\langle\Sigma_{\text{f}}\rangle$ and $\langle\Sigma_{\text{c}}\rangle$ the average macroscopic fission and capture cross sections, $\langle v\rangle$ the average speed of a neutron and DB^2 the leakage term [2].

Let us define the average intergeneration time l as the average time between a fission and the previous one in the chain reaction. In the case of one group point kinetics, it is precisely the lifetime of a neutron (because the fission probability is independent of the age of the neutron). It is given by

$$l = \frac{1}{\left(\langle\Sigma_{\text{f}}\rangle + \langle\Sigma_{\text{c}}\rangle + DB^2\right)\langle v\rangle}$$

A discussion on different definitions of the lifetime can be found in [9].

4

The multiplication coefficient is

$$k_{\text{eff}}^{\text{P}} = \frac{\nu_{\text{p}}\langle\Sigma_{\text{f}}\rangle}{\langle\Sigma_{\text{f}}\rangle + \langle\Sigma_c\rangle + DB^2} = \nu_p l \langle\Sigma_f\rangle\langle v\rangle$$

The one group point kinetics leads to an exponential decrease of the population with a constant decrease rate Ω defined as follows :

$$-\frac{1}{N}\frac{dN}{dt} = \Omega(t) \equiv \Omega = \frac{1 - k_{\text{eff}}^{\text{P}}}{l}$$

Of course the flux, and any reaction rate will follow the same decrease.

Thus, if we are able to determine l by simulation (it cannot be measured directly), the one group point kinetics allows us to deduce $k_{\text{eff}}^{\text{P}}$ from a measurement of the decrease rate Ω supposed to be constant in time.

2.2   The real decrease

Let us compare this conclusion with a "real decrease", simulated with the Monte-Carlo code MCNP4B[1], for a spherical fast reactor with $k_{\text{eff}}^{\text{P}} = 0.972$, composed of a 90 cm diameter core made of 27 % Pu MOX, surrounded by a 20 cm thick sodium/stainless steel reflector. It will be our reference reactor.

In the simulations $\Omega(t)$ is defined as the decrease rate of the total fission rate $N_{\text{f}}(t)$ rather than the neutron population $N(t)$:

$$\Omega(t) = \frac{1}{N_{\text{f}}}\frac{dN_{\text{f}}}{dt}$$

We will see in section 3 the reasons why $N_{\text{f}}(t)$ is chosen instead of $N(t)$. According to point kinetics, $N(t)$ is proportional to $N_{\text{f}}(t)$ as $N_{\text{f}}(t) = N(t)\langle\Sigma_{\text{f}}\rangle\langle v\rangle$, so the definition of $\Omega(t)$ is not affected by the use of either $N(t)$ or $N_{\text{f}}(t)$.

The result is shown in figure 1. $\Omega(t)$ appears not to be a constant, but goes towards an asymptotic value Ω_∞ after a very long time (~ 200 μs whereas $l = 0.3$ μs), when very few neutrons remain in the reactor. Therefore this asymptotic decrease rate Ω_∞ is not accessible to experiment. Moreover, Ω_∞ is different from $(1 - k_{\mathrm{eff}}^{\mathrm{P}})/l$, and we will see in section 3.2.3 that there is no simple relation between them.

2.3   Role of the reflector

Let us try to understand in which circumstances such an unpleasant behaviour arises. The only way to account for such long times is to consider the role of the reflector. While the one group point kinetics implies an exponential distribution for intergeneration times, in an actual reactor neutrons may spend a lot of time in the reflector, where absorption cross sections are low, before coming back into the fuel. These few long-life neutrons appear to have a major impact on the kinetics of the system, in the same way as the delayed neutrons, but with an intermediate time scale.

It is possible to check this effect by considering another reactor with the same size and the same reactivity, comprising only the fuel. A greater proportion of plutonium in the MOX is used to compensate for the loss of reactivity. The result shown in figure 2 confirms our assumption : point kinetics results are not far from the asymptotic decrease rate, which is reached within only a few microseconds, while $l = 0.1$ μs.

Figure 3 shows the case of a larger reactor (170 cm diameter spherical core surrounded by the same reflector as the reference reactor), again at $k_{\mathrm{eff}}^{\mathrm{P}} =$

0.972. The impact of the reflector on the kinetics decreases with the size of the reactor. This means that a large power reactor would be easier to describe than a small experimental reactor.

2.4 Role of the subcriticality

It is easy to understand that the presence of the reflector introduces long time scales for one generation. But how does this induce long time scales for the whole decrease ?

As a matter of fact, long-life neutrons constitute a very small fraction of the total number of neutrons. If all generations are present at the same time, few old neutrons of first generations will be mixed with many young neutrons of later generations and will not have a noticeable impact on the whole decrease. On the contrary, if only few first generations of neutrons are present after a while, these long-life neutrons will represent a significant proportion of the population.

Now, the competition between different generations is controlled by the level of subcriticality, since the nth generation is weighted by $k_{\text{eff}}^{\text{P}}{}^{n}$. This effect is shown figure 4 for our reference reactor at $k_{\text{eff}}^{\text{P}} = 1.0$ and $k_{\text{eff}}^{\text{P}} = 0.9$, after $30 \, \mu\text{s} = 100 \, l$. For $k_{\text{eff}}^{\text{P}} = 1.0$, generations follow a gaussian distribution centered on 100. For $k_{\text{eff}}^{\text{P}} = 0.9$, nearly all neutrons belong to generations less than 50. This shows that the influence of the long-life neutrons increases dramatically with the level of subcriticality. The greater the subcriticality, the older the neutrons present at a given time. In the same way, a growing human population will be mainly young, while a small birth rate will lead to an older population.

Figure 5 shows the decrease rate $\Omega(t)$ for a slightly subcritical (-600 pcm) version of the reference reactor, obtained by increasing the Pu proportion in the MOX, confirming the above conclusion: in that case point kinetics gives a reasonably good result.

3   The intergeneration time distribution $P(\tau)$

It appears that in the case of a small reactor with a reflector and a large subcriticality, long life neutrons have to be taken into account.

We introduce the intergeneration time distribution $P(\tau)$, defined as the distribution of times between the birth of a neutron by fission and the previous one in the chain reaction.

It satisfies

$$\int_0^\infty P(\tau)d\tau = k_{\text{eff}}^{\text{p}} \tag{1}$$

$$\int_0^\infty \tau P(\tau)d\tau = k_{\text{eff}}^{\text{p}}\, l \tag{2}$$

where (1) expresses that each fission induces $k_{\text{eff}}^{\text{p}}$ other fissions at the next generation.

(2) expresses that the mean intergeneration time is l. l is merely the first moment of the distribution $P(\tau)$, and does not contain any information on the shape of $P(\tau)$.

We will work under the assumption that all the fissions are equivalent. In particular this distribution $P(\tau)$ is the same for every fission occuring in the

8

reactor fuel.

This is a less restrictive assumption than the assumption of equivalent neutrons that underlies the one group point kinetics : here the neutrons can have different properties depending on the time τ elapsed since their birth by fission (or their emission by the source). At a given time, every neutron is thus characterized by this variable τ.

For these reasons we consider that the right parameter to monitor is $N_\mathrm{f}(t)$ rather than $N(t)$, and we will use it to define $\Omega(t)$.

3.1   Kinetic equations using $P(\tau)$

Under this assumption, $P(\tau)$ entirely determines the reactor kinetics. If $N_\mathrm{f}(t)$ is the fission rate at time t, $N_\mathrm{f}(t)$ can be deduced from N_f at earlier times through the equation :

$$N_\mathrm{f}(t) = \int_0^\infty N_\mathrm{f}(t - \tau)P(\tau)d\tau \tag{3}$$

Which leads for a dirac pulse to :

$$N_\mathrm{f} = P + P * P + P * P * P + \ldots \tag{4}$$

where the star denotes convolution.

Assuming that the decrease rate tends to an asymptotic value Ω_∞, that value can be deduced from (3) by replacing $N_\mathrm{f}(t)$ by $e^{-\Omega_\infty t}$. It satisfies :

$$\int_0^\infty e^{\Omega_\infty \tau} P(\tau)d\tau = 1 \tag{5}$$

Since the above integral is an increasing function of Ω_∞, Ω_∞ can be easily calculated by dichotomy, as it has been done in figure 1.

3.2 Some results for Ω_∞

3.2.1 Two simple cases

The point kinetics leads to an exponential distribution for intergeneration times :

$$P(\tau) = \frac{k_{\mathrm{eff}}^{\mathrm{P}}}{l} e^{-\tau/l} \;\Rightarrow\; \Omega_\infty = \frac{1 - k_{\mathrm{eff}}^{\mathrm{P}}}{l}$$

An even simpler case is the one where all the neutrons have precisely the same life time :

$$P(\tau) = k_{\mathrm{eff}}^{\mathrm{P}} \delta(\tau - l) \;\Rightarrow\; \Omega_\infty = -\frac{\ln(k_{\mathrm{eff}}^{\mathrm{P}})}{l}$$

3.2.2 Upper limit of Ω_∞

If we define

$$I_P(\Omega) = \int_0^\infty e^{\Omega\tau} P(\tau) d\tau$$

(5) can be rewritten as

$$I_P(\Omega_\infty) = 1$$

Let us now define

$$I'_P(\Omega) = \int_0^\infty e^{\Omega l}(\Omega(\tau - l) + 1)P(\tau)d\tau$$

10

As $e^{\Omega l}(\Omega(\tau - l) + 1) \leq e^{\Omega \tau}$ with a common tangent at $\tau = l$, we have :

$$I'_P(\Omega) \leq I_P(\Omega)$$

(1) and (2) imply

$$I'_P(\Omega) = k^{\mathrm{P}}_{\mathrm{eff}} e^{\Omega l}$$

So

$$I_P(\Omega) \geq k^{\mathrm{P}}_{\mathrm{eff}} e^{\Omega l}$$

Let us take $\Omega = -\ln(k^{\mathrm{P}}_{\mathrm{eff}})/l$. We obtain

$$I_P\left(-\frac{\ln(k^{\mathrm{P}}_{\mathrm{eff}})}{l}\right) \geq 1 = I_P(\Omega_\infty)$$

As $I_P(\Omega)$ is an increasing function of Ω, we can give an upper limit for Ω_∞ :

$$\Omega_\infty \leq -\frac{\ln(k^{\mathrm{P}}_{\mathrm{eff}})}{l}$$

The decrease is always slower than in the case where all the neutrons have the same lifetime. Usually, it is even slower than the point kinetics prediction.

3.2.3   Developing Ω_∞ near $k^{\mathrm{P}}_{\mathrm{eff}} = 1$

If in (5), we develop $e^{\Omega \tau}$ around $\tau = 0$, it is easy to prove that :

$$1 = \int_0^\infty P(\tau)d\tau + \Omega_\infty \int_0^\infty \tau P(\tau)d\tau + \frac{\Omega_\infty^2}{2} \int_0^\infty \tau^2 P(\tau)d\tau$$
$$+ \frac{\Omega_\infty^3}{6} \int_0^\infty \tau^3 P(\tau)d\tau + \dots$$

11

which can be divided on both sides by $k_{\mathrm{eff}}^{\mathrm{P}}$:

$$1 + (1 - k_{\mathrm{eff}}^{\mathrm{P}}) + (1 - k_{\mathrm{eff}}^{\mathrm{P}})^2 + (1 - k_{\mathrm{eff}}^{\mathrm{P}})^3 + \ldots$$
$$= 1 + \Omega_\infty \langle \tau \rangle + \frac{\Omega_\infty^2}{2} \langle \tau^2 \rangle + \frac{\Omega_\infty^3}{6} \langle \tau^3 \rangle + \ldots$$

This leads to

$$\Omega_\infty = (1 - k_{\mathrm{eff}}^{\mathrm{P}}) \, \frac{1}{\langle \tau \rangle} + (1 - k_{\mathrm{eff}}^{\mathrm{P}})^2 \, \frac{2 \langle \tau \rangle^2 - \langle \tau^2 \rangle}{2 \langle \tau \rangle^3}$$
$$+ (1 - k_{\mathrm{eff}}^{\mathrm{P}})^3 \, \frac{6 \langle \tau \rangle^4 - 6 \langle \tau \rangle^2 \langle \tau^2 \rangle + 3 \langle \tau^2 \rangle^2 - \langle \tau^3 \rangle \langle \tau \rangle}{6 \langle \tau \rangle^5} + \ldots$$

Let us now introduce the moments of the distribution $P(\tau)$, mean $\langle \tau \rangle = l$, variance $\langle \tau^2 \rangle - \langle \tau \rangle^2 = \sigma^2$ and skewness $\langle (\tau - l)^3 \rangle / \sigma^3 = y$:

$$\Omega_\infty = \frac{1 - k_{\mathrm{eff}}^{\mathrm{P}}}{l} + \frac{(1 - k_{\mathrm{eff}}^{\mathrm{P}})^2}{2l} \left(1 - \frac{\sigma^2}{l^2} \right)$$
$$+ \frac{(1 - k_{\mathrm{eff}}^{\mathrm{P}})^3}{6l} \left(2 - y \frac{\sigma^3}{l^3} - 3 \frac{\sigma^2}{l^2} \left(1 - \frac{\sigma^2}{l^2} \right) \right) + \ldots \tag{6}$$

The point kinetics prediction is only the first order in $1 - k_{\mathrm{eff}}^{\mathrm{P}}$ of the exact value of Ω_∞. The terms in $(1 - k_{\mathrm{eff}}^{\mathrm{P}})^n$ involve up to the nth moment of the distribution $P(\tau)$.

The above formula shows that the knowledge of l is not sufficient and that there is no simple link between $k_{\mathrm{eff}}^{\mathrm{P}}$ and Ω_∞. Therefore Ω_∞ is not the relevant quantity to measure in order to determine $k_{\mathrm{eff}}^{\mathrm{P}}$.

4 The proposed method

It appears that the decrease, in the general case, cannot be characterized by a single decrease rate. Besides, even if we had experimental access to the

12

asymptotic decrease rate, it would not give us much information concerning $k_{\text{eff}}^{\text{P}}$.

We will then choose to measure the decrease $\Omega(t)$ as a function of time, and compare it with simulations for different $k_{\text{eff}}^{\text{P}}$.

Simulating many decreases for many similar reactors with slightly different $k_{\text{eff}}^{\text{P}}$ is awfully time consuming and introduces arbitrary modifications of the reactor to make $k_{\text{eff}}^{\text{P}}$ vary. Instead, we propose here to simulate only the intergeneration time distribution $P(\tau)$ and deduce from it the decrease rate for any value of $k_{\text{eff}}^{\text{P}}$, by convolving $P(\tau)$ with itself, as many times as necessary, according to (4).

4.1 Application to the reference reactor

The first step is to normalize $P(\tau)$ to $k_{\text{eff}}^{\text{P}} = 1$ by computing :

$$P'(\tau) = \frac{P(\tau)}{\int_0^\infty P(u)du} \tag{7}$$

Then, for any given value of $k_{\text{eff}}^{\text{P}}$, we can compute the fission rate

$$N_{\text{f}k_{\text{eff}}^{\text{P}}}(t) = k_{\text{eff}}^{\text{P}} P' + k_{\text{eff}}^{\text{P}}{}^2 P' * P' + k_{\text{eff}}^{\text{P}}{}^3 P' * P' * P' + \ldots \tag{8}$$

And finally, the decrease rate, function of time

$$\Omega_{k_{\text{eff}}^{\text{P}}}(t) = \frac{1}{N_{\text{f}k_{\text{eff}}^{\text{P}}}} \frac{dN_{\text{f}k_{\text{eff}}^{\text{P}}}}{dt}$$

Knowing the real decrease rate $\Omega(t)$ from the experimental data, it is possible to fit it by $\Omega_{k_{\text{eff}}^{\text{P}}}(t)$, which provides us with the parameter $k_{\text{eff}}^{\text{P}}$. Of course, the

better $\Omega_{k_{\text{eff}}^{\text{P}}}(t)$ fits $\Omega(t)$, the more reliable the result is.

As we do not have experimental data yet, the "real" decreases have also been simulated for four different proportions of plutonium in our reference reactor, giving $k_{\text{eff}}^{\text{P}} = 0.963$, $k_{\text{eff}}^{\text{P}} = 0.972$, $k_{\text{eff}}^{\text{P}} = 0.984$, $k_{\text{eff}}^{\text{P}} = 0.994$, with a central source of 2.5 MeV neutrons.

The fit has been performed from 5 μs (to let the system forget the characteristics of the source) to 40 μs (to avoid dealing with the delayed neutrons), far before reaching the asymptotic value Ω_∞.

Figure 6 shows these decreases, with their error bars, together with the results of the fits (smooth lines). $\Omega_{k_{\text{eff}}^{\text{P}}}(t)$ are also shown for 100 pcm more and 100 pcm less than the value of $k_{\text{eff}}^{\text{P}}$ given by the fit, in order to show the sensitivity of the method.

The agreement is quite good but not perfect. The values of $k_{\text{eff}}^{\text{P}}$ provided by the fits lead to a knowledge of $1 - k_{\text{eff}}^{\text{P}}$ with a precision of around 15% in each case. This can be seen on figure 8. The fact that the error is proportional to $1 - k_{\text{eff}}^{\text{P}}$ rather than $k_{\text{eff}}^{\text{P}}$ is not surprising, in view of equation (6) for example, but it is a very important point for safety issues : the more critical the reactor becomes, the more reliable the measure of $k_{\text{eff}}^{\text{P}}$ becomes.

4.2 Improving the method

In order to improve the agreement, we now have to reconsider the only assumption we made, which was the equivalence of every fission.

More precisely, we will consider different P distributions for fissions occuring

14

after different times τ. Let $P_{\tau_1}(\tau_2)$ be the distribution of intergeneration times τ_2, if the first of the two fissions considered occured itself a time τ_1 after the previous one.

The distribution $P_{\tau_1}(\tau_2)$ varies with τ_1 both in shape and in integral value.

To understand this change, we can consider what happens to the neutrons of a single generation. Some neutrons are quickly captured in the fuel, while others spend some time in the reflector, where they are progressively slowed down. The longer they stay in the reflector, the slower they are, the larger the capture cross sections become, and the more the corresponding fissions occur at the peripheral part of the fuel. These late superficial fissions produce neutrons that have a higher probability to escape, and a slightly longer lifetime.

We cannot afford to take into account the variations in the shape of the P distribution, which would imply very heavy simulations and calculus. Moreover, making the assumption that this shape is constant is a quite reasonable approximation, as we will see below. Therefore we define

$$I(\tau_1) = \frac{\int_0^\infty P_{\tau_1}(\tau_2)d\tau_2}{\int_0^\infty P(\tau)d\tau}$$

and we assume that we can write $P_{\tau_1}(\tau_2) = I(\tau_1)P(\tau_2)$. $I(\tau_1)$ is proportional to the total number of fissions induced by the first one. It can be understood as the relative importance of this fission.

Our new model is the following : the only characteristic that differs from fission to fission is the importance, depending only on the time between the fission and the previous one in the chain.

Now, the terms we have to compute are convolutions of the form :

15

$$\int\limits_{\sum_{i=1}^n \tau_i = \tau} P(\tau_1)P_{\tau_1}(\tau_2)P_{\tau_2}(\tau_3)\ldots P_{\tau_{n-1}}(\tau_n)d\tau_1 d\tau_2 d\tau_3 \ldots d\tau_{n-1}$$

$$\int\limits_{\sum_{i=1}^n \tau_i = \tau} P(\tau_1)I(\tau_1)P(\tau_2)I(\tau_2)P(\tau_3)\ldots I(\tau_{n-1})P(\tau_n)d\tau_1 d\tau_2 d\tau_3 \ldots d\tau_{n-1}$$

Then if we define P'' like P' in (7) but weighted by the importance :

$$P''(\tau) = \frac{P(\tau)I(\tau)}{\int_0^\infty P(u)I(u)du}$$

Equation (8) becomes

$$N_{f k_{\text{eff}}^{\text{p}}}(t) = k_{\text{eff}}^{\text{p}} P' + k_{\text{eff}}^{\text{p}}{}^2 P'' * P' + k_{\text{eff}}^{\text{p}}{}^3 P'' * P'' * P' + \ldots$$

The other steps are left unchanged. The new fits are shown figure 7.

The new fits seem more reliable, especially for small values of $k_{\text{eff}}^{\text{p}}$. The results are summarized in figure 8, which shows, for the different levels of subcriticality, the error in the determination of $k_{\text{eff}}^{\text{p}}$ as given by the two methods. It appears that the improved method using the importance gives very good results, almost within the statistical error.

5   Robustness of the method

We have to evaluate the robustness of the method through its different stages, simulation and experiment:

- The simulated $P(\tau)$ must be independent of small errors in the description of the reactor, while computing $k_{\text{eff}}^{\text{p}}$ directly would not.
- The measured $\Omega(t)$ must be independent of the neutron source and of the detecting device.

The $P(\tau)$ distribution has been calculated for various reactors derived from the reference reactor by changing either the proportion of plutonium in the core, or the diameter of the core, keeping always the same reflector. The $k_{\mathrm{eff}}^{\mathrm{P}}$ varies in a range from 0.957 to 1.000. In order to compare them, each $P(\tau)$ distribution has been normalized to $k_{\mathrm{eff}}^{\mathrm{P}} = 1$. The result is shown in figure 9.

The perfect superposition of the distributions confirms our assumption that it is independent of small errors in the description of the core.

Even the small correction applied by weighting $P(\tau)$ by the importance $I(\tau)$ presents the same characteristics of robustness.

The oscillations in the distributions previously plotted can be explained by the variations of the spectrum of neutrons coming back from the reflector into the core, already mentioned in subsection 4.2. As the mean energy of neutrons coming back decreases, the fission/capture cross section ratio changes and reproduces precisely the observed oscillations.

If we now study the effect of the reflector on the shape of $P(\tau)$, for example by varying the thickness of the reflector, as in figure 10, we observe that the proportion of long-life neutrons is slightly increased, as well as the mean intergeneration time l.

We have in the system two different characteristic times. In the fuel, the neutrons have a very short lifetime, of several hundreds of nanoseconds. In the reflector, they can live several tens of microseconds. As we are interested in time scales of tens of microseconds, the neutron lives in the fuel can be treated

as instantaneous. It is the reason why the precise size and composition of the core have a very small impact on the shape of $P(\tau)$, even if they have a great impact on $k_{\text{eff}}^{\text{p}}$. On the other hand, a reasonably precise description of the reflector appears to be necessary in order to get the correct $P(\tau)$ distribution. Other parts of the reactor with long time scales such as a lead target, a moderator,... would also be of importance.

This comment is of particular importance because along the life of a reactor, the variations of $k_{\text{eff}}^{\text{p}}$ are likely to come only from variations of the composition of the fuel due to burn-up and poisoning, but we don't expect variations of the reflector characteristics. In that case, even if $k_{\text{eff}}^{\text{p}}$ varies a lot, the distribution $P(\tau)$ will stay as constant as in figure 9, and a method based on $P(\tau)$ to determine $k_{\text{eff}}^{\text{p}}$ will prove very reliable.

5.2 Robustness of $\Omega(t)$

Calculations of the decrease rates of the total fission rate have been performed for four different sources, central, peripheral or distributed, of various energies, and for four different reactors, each one with a different value of $k_{\text{eff}}^{\text{p}}$. The results are shown figure 11. It appears that $\Omega(t)$, after few microseconds, is independent of the source and characterizes each reactor well.

But we cannot have experimental access to the total fission rate, since a neutron does not produce a signal in the detector just after its birth by fission. It is necessary here to introduce the distribution of times between the last fission and the signal in the detector. Let $D(\tau)$ be this new distribution. The measured quantity is N_{m} therefore the result of a last convolution : $N_{\text{m}} = N_{\text{f}} * D$.

For some detectors, the $D(\tau)$ distribution will have a very small characteristic time in comparison with N_{f}. In that case, it is possible to make the approximation that $N_{\mathrm{m}}(t) = N_{\mathrm{f}}(t) \int_0^\infty D(\tau)d\tau$, and therefore the measured decrease rate is equal to the decrease rate of the total fission rate : the above method applies as is.

Typically, such detectors will either use a threshold-dependent reaction, or will lie well inside the core. In the first case, only fast neutrons will induce a signal, and fast neutrons are always "young" ones. In the second case, the detector is protected from slow neutrons coming back from the reflector by absorption in the external parts of the fuel. In both cases, the important point is that the detector can see only fast neutrons, either because of its intrinsic characteristics, or because of its location in the core.

The case of a threshold-dependent detector is particularly interesting for application to a power reactor, because it allows to place the detector inside the reflector, or anywhere where the neutron flux is not too high.

Figure 12 illustrates the two cases discussed above. It shows the simulation of such experimental data obtained by two central detectors and two threshold-dependent detectors in the reflector. The corresponding decrease rates fit with the total fission rate decrease rate within the limits of the statistical error.

On the contrary, a detector with a wide energy range placed in the reflector (or near to it) will show a very different decrease rate, as can be seen on figure 13.

But even in that case, it is still possible to apply our method. Nevertheless, the $D(\tau)$ distribution has to be simulated in addition to $P(\tau)$. It has been done

for a matter of demonstration for the U^{235} and He^3 detectors in the reflector, and the resulting fits are displayed on figure 13.

Once again, the fits are very good, and the obtained values $k_{\text{eff}}^{\text{P}} = 0.9713$ and $k_{\text{eff}}^{\text{P}} = 0.9711$ remain perfectly compatible with the one obtained directly from the total fission rate.

Like $P(\tau)$, the $D(\tau)$ distribution is very robust against small errors in the description of the core, and depends above all on the description of the detector itself (for the detecting cross sections) and of the reflector (introducing the long time scales).

Of course, avoiding this new distribution by using a threshold-dependent detector simplifies both the simulations and the calculations, and removes possible sources of errors. If it is not threshold-dependent, it is advisable to protect the detector from slow neutrons, for example by means of an absorbing shell. Nevertheless it is worth knowing that we can deal with many types of detectors, keeping a very good estimation of $k_{\text{eff}}^{\text{P}}$.

6 Conclusion

We propose a method for the experimental determination of $k_{\text{eff}}^{\text{P}}$ that is independent of the assumptions made in one group point kinetics calculations. It is built on the intergeneration time distribution, $P(\tau)$. This distribution is a relevant quantity to describe the prompt kinetics of the reactor. It is independent of small variations in the composition of the fuel, and is largely determined by the characteristics of the reflector. It can be easily and precisely computed by a Monte-Carlo simulation, provided the geometry and the composition of the

reflector are precisely known, and the cross section databases (in particular elastic scattering) are reliable.

The determination of $k_{\mathrm{eff}}^{\mathrm{p}}$ is achieved by fitting a measured decrease rate by a function calculated from $P(\tau)$. Better results can be obtained by weighting $P(\tau)$ by the importance of the corresponding fissions. The measured decrease rate is independent of the neutron source and of the detecting device after a very short time, as long as the detector is threshold-dependent or protected from slow neutrons.

We still have to validate this method with the experimental data of the upcoming MUSE 4 experiment. The major difference with the cases studied here lies in the complexity of the core. But no major change is expected in its kinetic behaviour. It would be also of interest to try and apply this method to thermal reactors, where the time scales are quite different.

As the decrease rates discussed here allow us to determine $k_{\mathrm{eff}}^{\mathrm{p}}$ in a never-critical assembly, and to check the description of the reactor and of the materials used in the simulation, through the accuracy of the fit, it suggests that subcritical assemblies could be powerful platforms for studying future reactor concepts, in a very safe and straightforward way.

References

[1] Judith F. Briesmeister. *MCNP - A General Monte-Carlo N Particle Transport Code.* Los Alamos Laboratory report LA-12625-M (1997)

[2] Karl O. Ott & Robert J. Neuhold. *Introductory Nuclear Reactor Dynamics.* American Nuclear Society, La Grange Park, Illinois (1985).

[3] Jean Bussac & Paul Reuss. *Traité de Neutronique.* Hermann (1985).

[4] Robert Barjon. *Physique des Réacteurs Nucléaires.* (1993).

[5] John R. Lamarsh & Anthony J. Baratta. *Introduction to Nuclear Engineering.* Third edition. Prentice Hall. (2001)

[6] Olivier Guéton. *Physique associée au contrôle et à la sûreté des systèmes hybrides.* Thesis presented in the University of Paris XI - Orsay. (2001)

[7] H. Nifenecker & al. *Hybrid Nuclear Reactors.* Progress in Part. & Nucl. Phys. 43 (1999) 683-827.

[8] Sylvain David. *Capacité des réacteurs hybrides au plomb pour la production d'énergie et l'incinération avec multirecyclage des combustibles. Evolution des paramètres physiques. Radiotoxicités induites.* Thesis presented in the University Joseph Fourier - Grenoble. (1999)

[9] M. Hayashi. *Comments on "Neutron Lifetime, Fission Time and Generation Time".* Nucl. Science and Engineering 121 (1995) 492

[10] C. Rubbia & al. *Conceptual design of a fast neutron operated high power energy amplifier* CERN/AT/95-44(ET). (1995)

List of Figures

23

Fig. 1. Decrease rate $\Omega(t)$ for the reference reactor, its asymptotic value Ω_∞ and the point kinetics value $(1 - k_{\mathrm{eff}}^{\mathrm{p}})/l$

Fig. 2. Decrease rate for the reflectorless reactor at $k_{\mathrm{eff}}^{\mathrm{p}} = 0.972$, and the point kinetics value
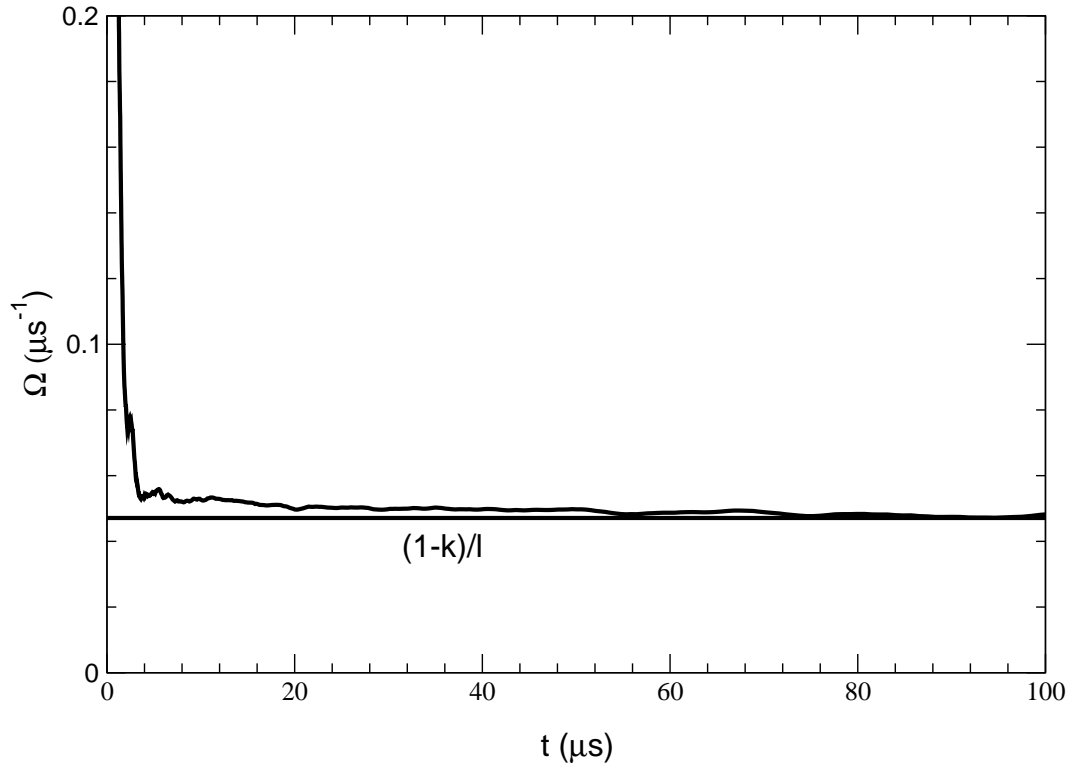
Fig. 3. Decrease rate for the bigger reactor (170 cm diameter core) at $k_{\mathrm{eff}}^{\mathrm{p}} = 0.972$, and the point kinetics value
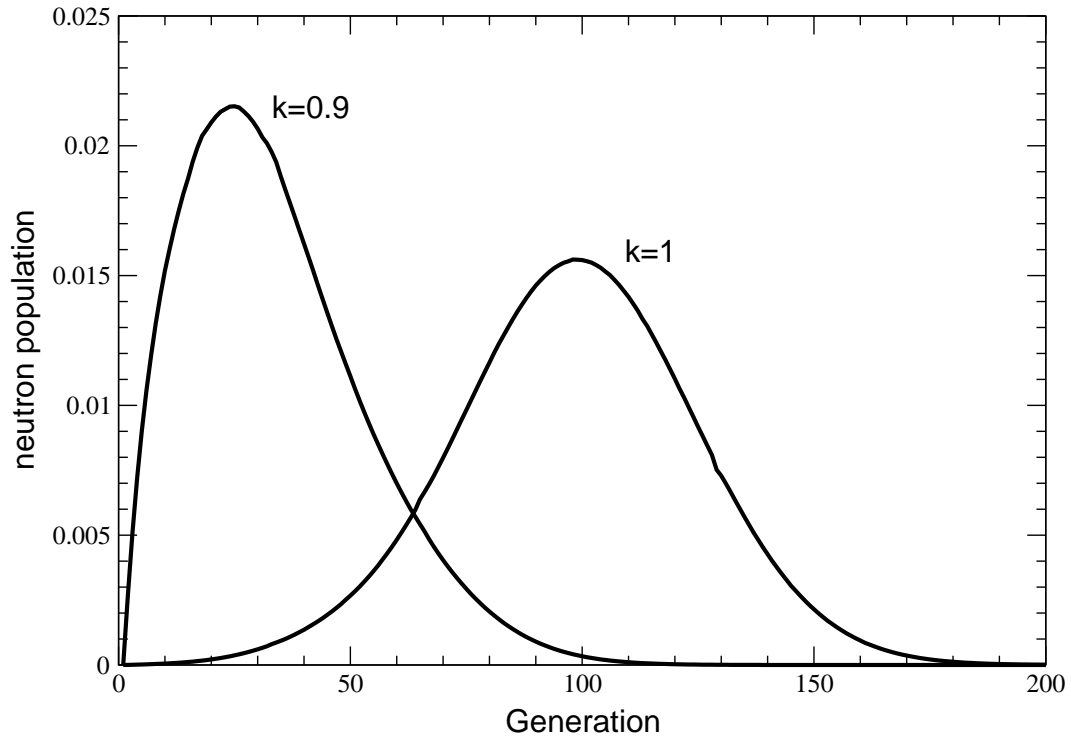
Fig. 4. Distribution of the generations of the fissions occuring at $t = 30\ \mu$s for the reference reactor at $k^{\mathrm{p}}_{\mathrm{eff}} = 1.0$ and $k^{\mathrm{p}}_{\mathrm{eff}} = 0.9$

28
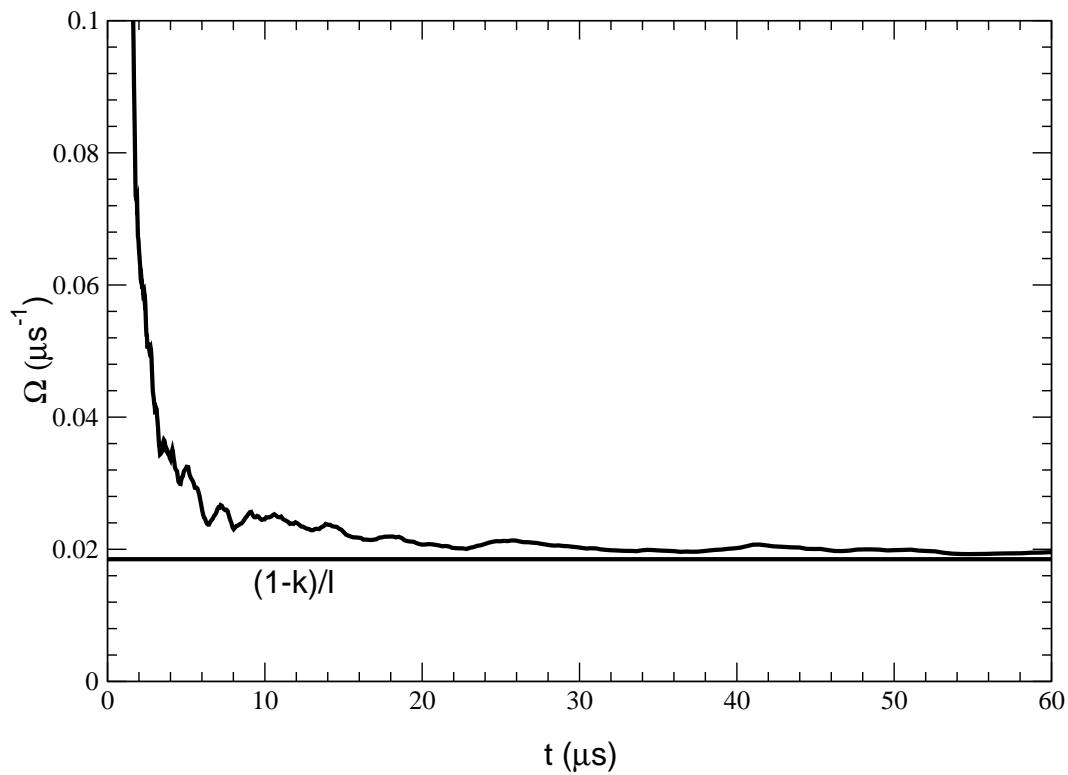
Fig. 5. Decrease rate for the reference reactor at $k_{\text{eff}}^{\text{p}} = 0.994$ (with 28% of Pu), and the point kinetics value
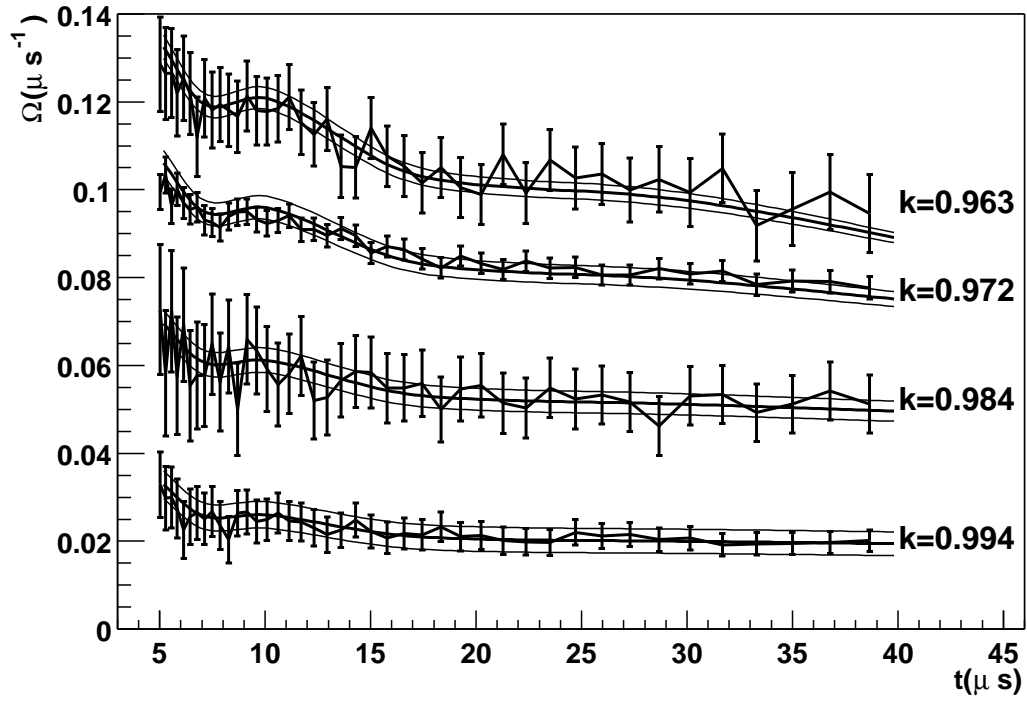
Fig. 6. $\Omega_{k_{\text{eff}}^{\text{p}}}(t)$ fits for 4 reactors of different $k_{\text{eff}}^{\text{p}}$. The polygonal lines with error bars show the "real" decreases while the smooth curves show the fit results, ± 100 pcm
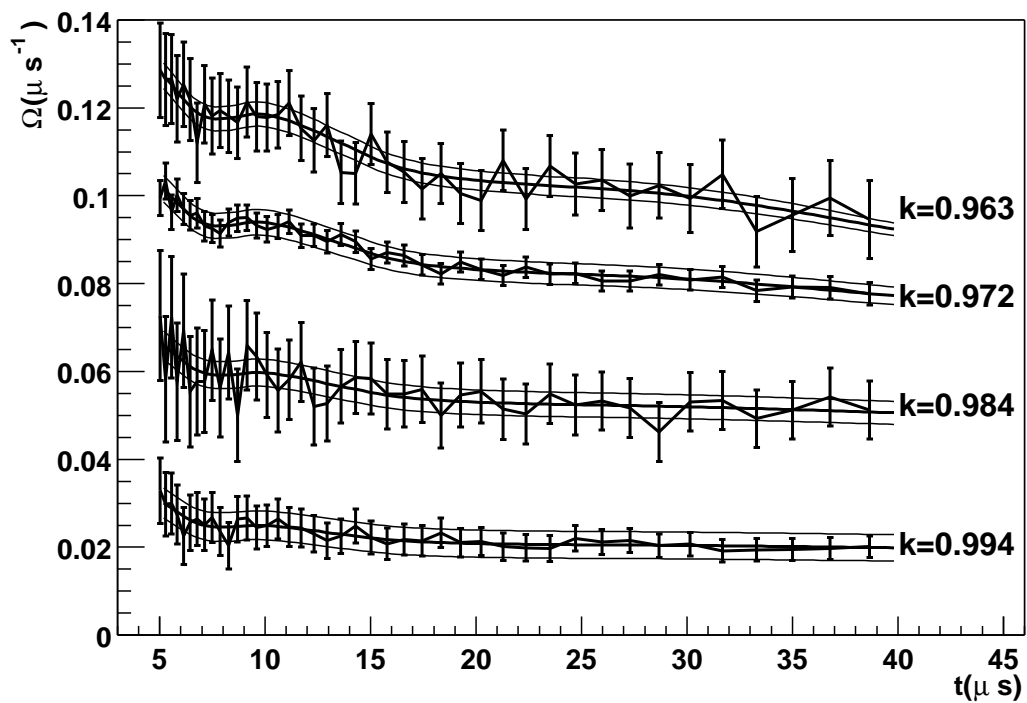
Fig. 7. $\Omega_{k_{\mathrm{eff}}^{\mathrm{p}}}(t)$ fits for 4 reactors of different $k_{\mathrm{eff}}^{\mathrm{p}}$, after weighting $P(\tau)$ by the importance
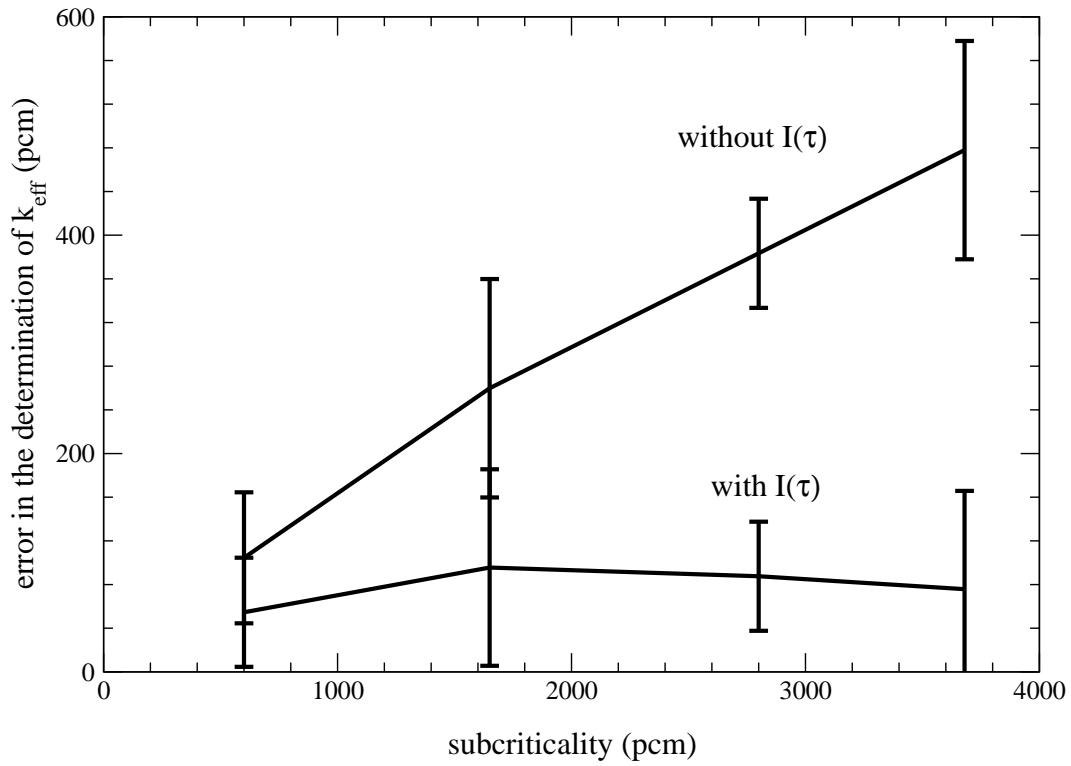
Fig. 8. Absolute errors in the determination of $k_{\mathrm{eff}}^{\mathrm{p}}$, function of $1 - k_{\mathrm{eff}}^{\mathrm{p}}$ with the two methods (with and without the importance weighting), and for the 4 different subcriticalities considered. The error bars show the statistical error
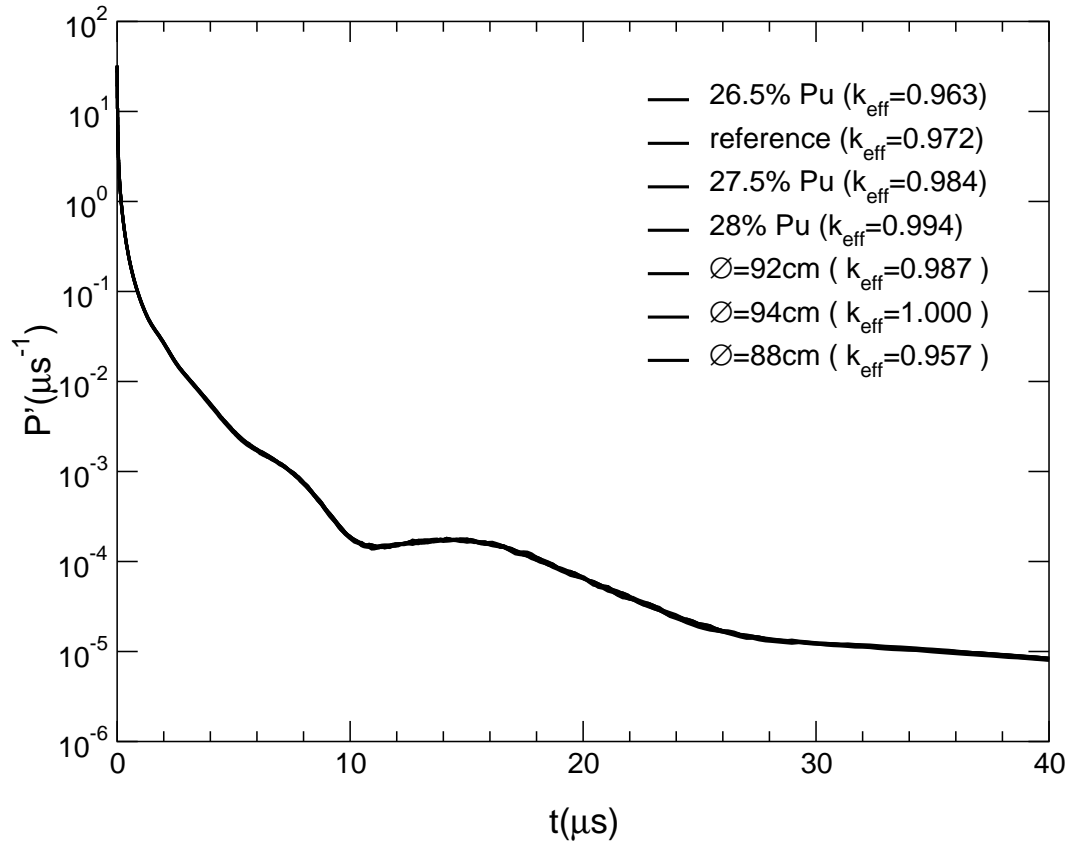
Fig. 9. Normalized $P(\tau)$ distribution for several variants of the reactor, with different $k_{\text{eff}}^{\text{p}}$ but the same reflector. One cannot distinguish the plots from one another.
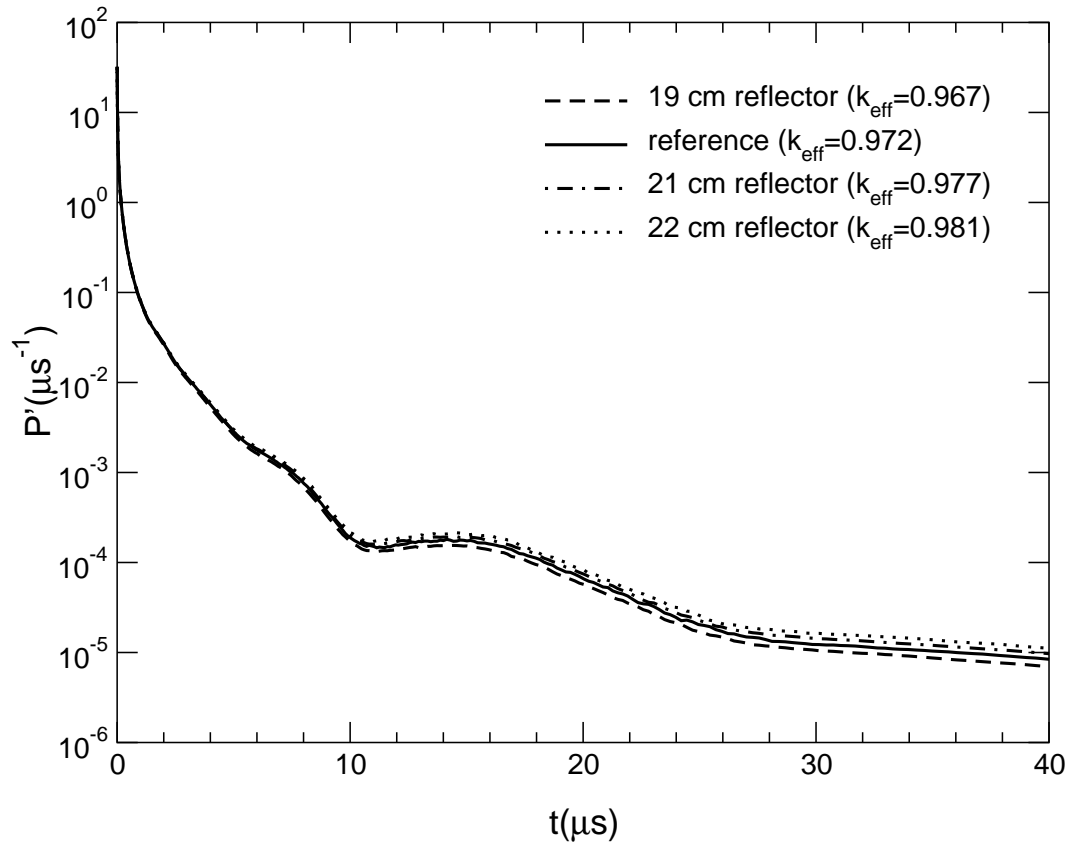
Fig. 10. Normalized $P(\tau)$ distribution for several thicknesses of the reflector
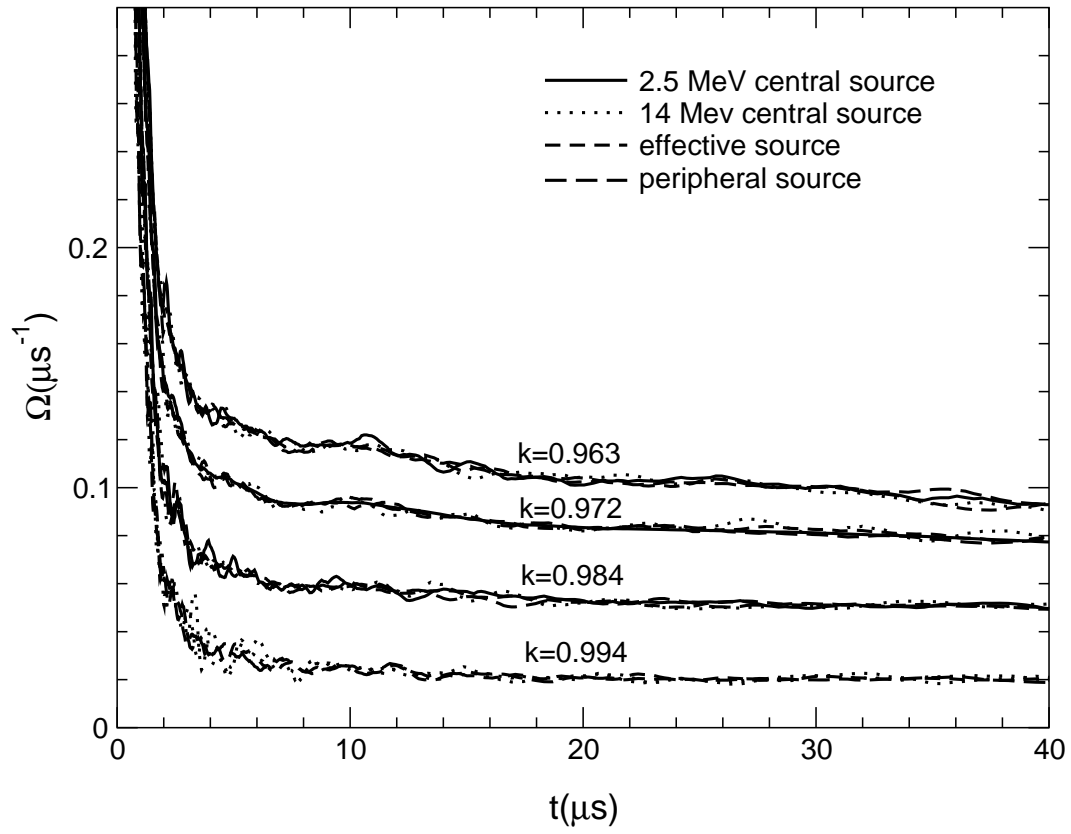
Fig. 11. Decrease rate of the total fission rate for 4 different sources and 4 different reactivities
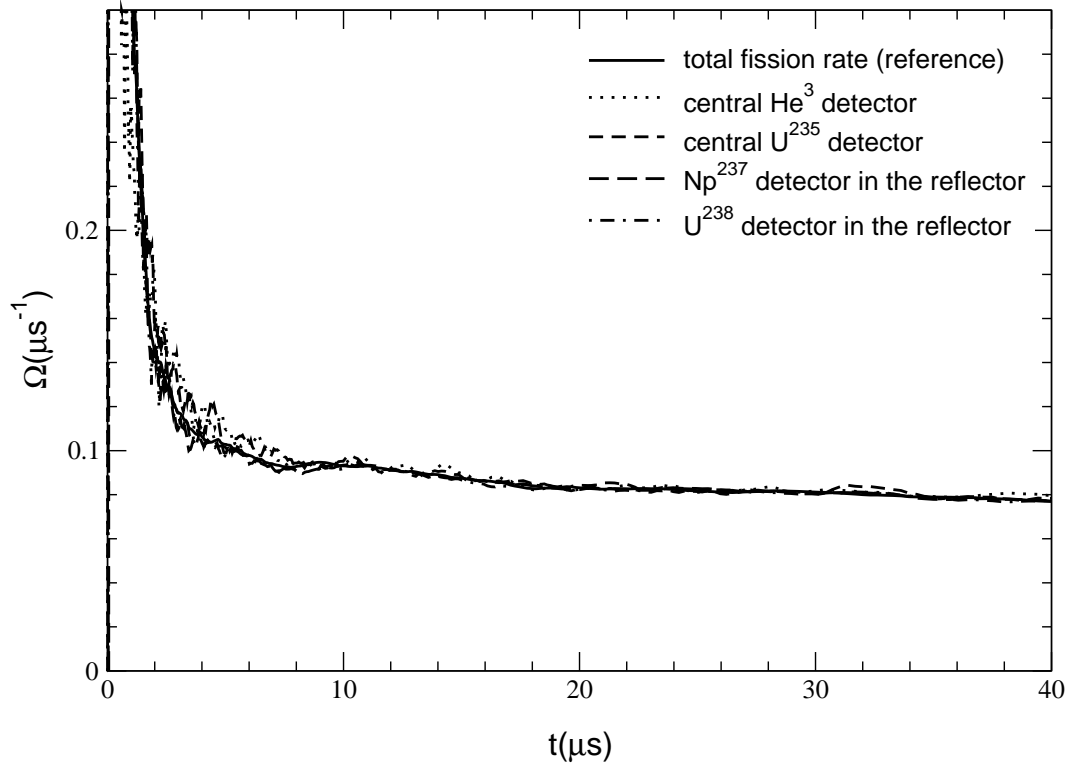
Fig. 12. Decrease rate of the signal given by a He^3 detector and a U^{235} fission chamber in the middle of the fuel, and by U^{238} and Np^{237} threshold-dependent fission chambers in the reflector
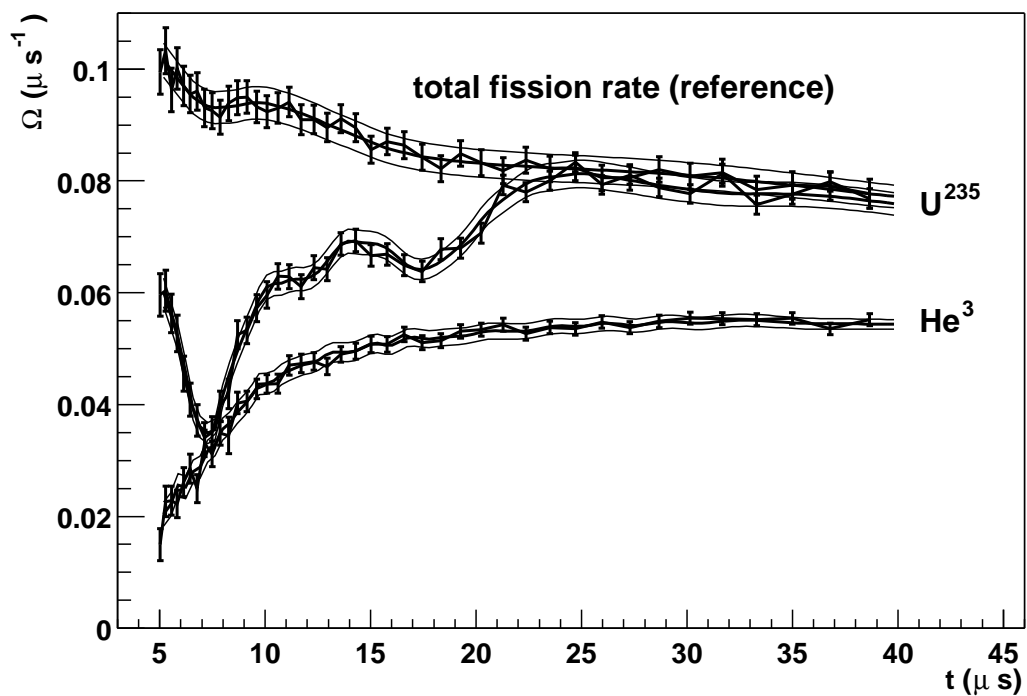
36

Fig. 13. Fits of the decrease rates of the signals given by U^{235} and He^3 detectors in the reflector, together with the decrease rate of the total fission rate, for the reference reactor